

Experimental Friction Coefficients for Bovine Cartilage Measured with a Pin-on-Disk Tribometer: Testing Configuration and Lubricant Effects

LIU SHI, VASSILIOS I. SIKAVITSAS, and ALBERTO STRIOLO

School of Chemical, Biological and Materials Engineering, The University of Oklahoma, Norman, OK 73019, USA

(Received 24 July 2010; accepted 15 September 2010; published online 25 September 2010)

Associate Editor Michael S. Detamore oversaw the review of this article.

Abstract—The friction coefficient between wet articular cartilage surfaces was measured using a pin-on-disk tribometer adopting different testing configurations: cartilage-on-pin vs. alumina-on-disk (CA); cartilage-on-pin vs. cartilage-on-disk (CC); and alumina-on-pin vs. cartilage-on-disk (AC). Several substances were dissolved in the phosphate buffered saline (PBS) solution to act as lubricants: 10,000 molecular weight (MW) polyethylene glycol (PEG), 100,000 MW PEG, and chondroitin sulfate (CS), all at 100 mg/mL concentration. Scanning electron microscopy photographs of the cartilage specimens revealed limited wear due to the experiment. Conducting the experiments in PBS solutions we provide evidence according to which a commercial pin-on-disk tribometer allows us to assess different lubrication mechanisms active in cartilage. Specifically, we find that the measured friction coefficient strongly depends on the testing configuration. Our results show that the friction coefficient measured under CC and AC testing configurations remains very low as the sliding distance increases, probably because during the pin displacement the pores present in the cartilage replenish with PBS solution. Under such conditions the fluid phase supports a large load fraction for long times. By systematically altering the composition of the PBS solution we demonstrate the importance of solution viscosity in determining the measured friction coefficient. Although the friction coefficient remains low under the AC testing configuration in PBS, 100 mg/mL solutions of both CS and 100,000 MW PEG in PBS further reduce the friction coefficient by ~40%. Relating the measured friction coefficient to the Hersey number, our results are consistent with a Stribeck curve, confirming that the friction coefficient of cartilage under the AC testing configuration depends on a combination of hydrodynamic, boundary, and weep bearing lubrication mechanisms.

Keywords—Articular cartilage, Friction coefficient, Testing configuration, Pin-on-disk tribometer.

Address correspondence to Alberto Striolo, School of Chemical, Biological and Materials Engineering, The University of Oklahoma, Norman, OK 73019, USA. Electronic mail: astriolo@ou.edu

INTRODUCTION

Osteoarthritis (OA) is a degenerative joint disease characterized by four main anatomical lesions: degenerative cartilage lesion (ulcerations tending ultimately to nude bone), proliferative lesion of the periosteum (bone osteophytes), degenerative bone lesion (subchondral bone sclerosis and subchondral bone lysis), and inflammatory lesion of the articular soft tissues (synovial effusion, edema, and progressive periarticular fibrosis). It affects nearly 5% of the general population and 80% of people over the age of 65,²⁴ with 27 million patients in the US alone.²⁵ Because one of the principal functions of cartilage is to provide support in diarthrodial joints, transmitting loads with minimum friction and wear,¹¹ it is likely that understanding the lubrication mechanism in healthy cartilage will lead to therapeutic strategies to relieve mild symptomatic OA, and possibly to improve the efficacy and expected lifetime of prosthetic implants. For this reason understanding the frictional properties of cartilage continues to be of enormous interest.

Although a number of experimental investigations report extremely low friction coefficients for cartilage, sometimes as low as ~0.01,¹⁴ the physiological mechanism responsible for such low friction coefficients is not completely understood. A number of hypotheses have been proposed, including fluid film lubrication mechanisms in the flavors of hydrodynamic,⁴³ elasto-hydrodynamic,¹⁶ squeeze-film,^{27,31,33} weeping,^{47,48} and boosted mechanisms,⁶⁹ boundary lubrication,^{17,35,46,62} and biphasic self-generating lubrication.^{1–5,15,41,44,52,53,58}

Among many factors that affect the friction coefficient for cartilage, such as sliding velocity, duration of load, loading rate, interfacial contact area, wear and so on, the presence of lubricants

appears to be essential to normal functioning of the joints.^{6,7,20,21,36,38–40,42,49,54,56,57,59,61,66} Hyaluronic acid (HA),^{7,19,50} phospholipids,^{19,61,63} chondroitin sulfate (CS),^{6,9,40} lubricin^{13,18,55}—the major components of natural synovial fluid (SF)—and polyethylene glycol (PEG)⁶ are reported to reduce the friction coefficient of articular cartilage. Although to explain these observations the boundary lubrication mechanism is often invoked, the mechanism by which each component present in SF facilitates lubrication, by itself or in combination with others, is not completely understood. Gleghorn and Bonassar²² showed that friction coefficients measured under various experimental conditions fall within a universal Stribeck curve, which satisfactorily relates the friction coefficient with shaft rotation rate and normal load. In the classic Stribeck curve, the measured friction coefficient is a function of the Hersey number, $\eta v/N$, where η is the dynamic viscosity of the lubricant solution, v the sliding velocity, and N is the normal load.²⁶ We are not aware of any systematic study in which the Hersey number is varied by changing the viscosity of the solution in which the experiments are conducted, while keeping all other parameters constant. Some literature reports have however addressed the effect of viscosity on the measured friction coefficients, and somewhat controversial results have been reported. For example, Mori *et al.*⁵⁰ found that very viscous HA lubricant solutions decrease the measured friction coefficient. Others found that the measured friction coefficient does not depend on the solution viscosity.⁶ Benz *et al.*⁸ reported that the viscosity of a fluid film containing HA is lower near the cartilage surface than in the bulk, suggesting that HA may not actually adsorb on the cartilage surface. One source of uncertainty may be related to the fact that most fluids in which the friction coefficient for cartilage is measured (e.g., the SF) are non-Newtonian. Thus, the viscosity used for calculating the Hersey number could be either the viscosity at a certain shear rate, or the zero-shear-rate viscosity.^{6,50}

To rationalize these observations it helps remembering that articular cartilage is a complex tissue. Cartilage shows a heterogeneous structure divided in four layers that differ in biochemical composition and molecular organization. The structural integrity of cartilage is probably responsible for its mechanical properties. In a simplistic description, cartilage can be pictured as a sponge in which a solid, highly charged phase provides support and confines a fluid phase within small cavities.⁶⁸ When a load is applied to cartilage the fluid is pumped out of the pores. McCutchen⁴⁸ provided evidence suggesting that, while inside the pores, the interstitial fluid contributes

to maintain low friction coefficients in cartilage. Hlavacek reported that the fluid escaping the pores yields a film on cartilage that quickly depletes, leaving the bearing surfaces into contact.^{28–34} When the fluid film is incomplete, lubrication is provided by the interstitial fluid. When the fluid film is intact lubrication is provided by fluid-film hydrodynamics. Ateshian *et al.* related the time-dependent friction coefficient to the interstitial fluid pressurization^{2,41}:

$$\mu_{\text{eff}}(t) = \left[1 - (1 - \varphi) \frac{W^P(t)}{W(t)} \right] \mu_{\text{eq}}. \quad (1)$$

In Eq. (1), $W(t)$ is the applied load and $W^P(t)$ is the load supported by the interstitial fluid, hence $W^P(t)/W(t)$ is the fraction of the load supported by the interstitial fluid; φ is the fraction of the cartilage surface that is solid and provides contact between two sliding surfaces; $\mu_{\text{eff}}(t)$ is the time-dependent friction coefficient; μ_{eq} is the friction coefficient at ‘steady-states,’ achieved after the two surfaces slide on each other for a long time. The interstitial fluid can support 90% or more of the total normal load ($W^P(t)/W(t)$), depending on the solicitation. This support can reduce to zero under prolonged static loading, at ‘steady-states’ conditions.

During activities such as walking and running the loading environment in the lower limbs is cyclical, allowing the SF to support large loads for short intervals and to replenish the cartilage before the load applies again on any contact area.^{2,60} McCutchen⁴⁸ reported that allowing a cartilage sample to replenish with SF for a few seconds was sufficient to restore low friction coefficients. Despite this, many available experimental data are collected under continuous static loads. One exception was reported recently by Caligaris and Ateshian,¹² who built a special tribometer with which they proved that when the contact area between two sliding cartilage surface moves (i.e., ‘migrating’ contact area), a constant, very low friction coefficient is observed. Measuring friction coefficients under conditions in which the contact area between the cartilage samples migrates is likely to mimic physiological conditions. Custom-made instruments, such as that designed by Caligaris and Ateshian, are suitable for such experiments, but it is possible that commercial pin-on-disk tribometers can provide the desired experimental conditions under appropriate testing configurations.

The objectives of the this study are (I) to assess whether a commercial pin-on-disk tribometer could be used to assess various lubrication mechanisms in articular cartilage; specifically, we seek to determine whether by changing the experimental set-up it is possible to establish experimental conditions under

which the contact area, the area on which the external load is applied, migrates on the cartilage substrate; (II) to determine the effect of solution viscosity toward reducing the measured friction coefficient; to this effect we dissolve different polymers in phosphate buffered saline (PBS) solutions; and (III) to interpret our experimental results invoking the interstitial fluid support (time-dependent friction coefficients) and the Stribeck curve (steady-states friction coefficients).

Although it is known that SF is an efficient lubricant, this fluid is not used in this study because it was preferred to control the solution composition by carefully measuring the concentration of two compounds (PEG and CS) within PBS solutions. These compounds change the solution viscosity. The effect on the measured friction coefficient of compounds such as lubricin and phospholipids, present in natural SF, will be considered in future studies.

Our results demonstrate that a commercial pin-on-disk tribometer can be used to measure the friction coefficient for articular cartilage over time under the precise control of sliding velocity and applied load. By controlling the experimental set-up, we propose a facile method to systematically probe different lubrication mechanisms. Mature bovine knee cartilage samples can be placed on the pin and/or on the disk, thus our technique is suitable for measuring friction coefficients for cartilage-on-pin vs. alumina-on-disk (CA), cartilage-on-pin vs. cartilage-on-disk (CC), and alumina-on-pin vs. cartilage-on-disk (AC) testing configurations. In the latter two testing configurations the contact area migrates on the cartilage surfaces, whereas the contact area remains constantly loaded in the CA testing configuration. Because configurations with migrating contact areas mimic the physiological cartilage behavior, they should yield low friction coefficients even when the experiments last for long times. In the second part of the article, using the AC testing configuration we demonstrate the importance of solution viscosity in determining the measured friction coefficient for articular cartilage.

MATERIALS AND METHODS

Cartilage Specimen Preparation

Bovine knees of age 15–30 months were purchased from Animal Technologies Inc. They were delivered within 3 days after slaughter. The knees were never frozen but stored at -4°C until dissection. Although cartilage degrades after slaughtering, scanning electron microscope (SEM) images show smooth surface structures, suggesting little, if any, surface cartilage degradation before testing. Full-depth osteochondral

plugs ($\varnothing = 12$ mm) were harvested from lateral and medial femoral condyles using a scalpel and 12 mm biopsy punches. The osteochondral plugs were trimmed to maintain a constant thickness (1.3 ± 0.2 mm) by removing the deep zone tissues with a sledge microtome (Leica SM2000 R), leaving the specimen surface intact. After preparation, the specimens were stored at -20°C in PBS solution (pH = 7.4, buffer strength = 150 mM). To maintain uniformity in our experiments, the osteochondral plugs were further cored out using biopsy punches to reduce the cylindrical cross section to $\varnothing = 10$ mm or $\varnothing = 2$ mm. The $\varnothing = 10$ mm specimens were glued to the disk and those with $\varnothing = 2$ mm were glued to the pins (details below) to perform lubrication experiments.

Lubricants Preparation

Articular joints are naturally immersed in SF. This fluid is a complex mixture containing HA, lubricin, phospholipids, and other compounds that contribute to lubrication, as well as to other biological functions. When our experiments in the AC testing configuration are conducted for cartilage immersed in natural SF, steady-states friction coefficients of 0.040 ± 0.004 are obtained under experimental conditions similar to those considered in this study (sliding speed of 1 mm/s and applied normal load of 2 N). These results are not discussed herein because, in an attempt to better understand the mechanism responsible for the low friction coefficients typically observed in cartilage, the lubricant composition is controlled as closely as possible, as described below.

In the simplest case, our experiments are conducted with the sliding surfaces immersed in PBS. To test the ability of different lubricants to reduce the friction coefficient for articular cartilage when dissolved in PBS, four different aqueous solution groups were prepared. Before testing cartilage samples were immersed in the corresponding solution for 12 h at 4°C after thawing. The control solution was PBS. The other three solutions were obtained by dissolving ‘lubricants’ in PBS. The lubricant solutions contained 100 mg/mL PEG of 10,000 molecular weight (MW) (Polymer Source, Inc., Dorval, QC, Canada), 100 mg/mL PEG of 100,000 MW (Sigma-Aldrich, St. Louis, MO, USA), and 100 mg/mL CS from shark cartilage (Sigma-Aldrich; CS molecular weight is not known). The ‘lubricants’ were used as-received. A SR5000 stress-controlled rheometer from Rheometric Scientific was used to measure the steady shear rate viscosity of each lubricant solution. The viscosity from each PBS solution was found to be constant over the shear rate range of $10\text{--}3000\text{ s}^{-1}$, indicating that the viscosity reached the zero-shear-rate limit. The zero-shear-rate

viscosity of PBS, 10,000 MW PEG, 100,000 MW PEG, and CS solutions at room temperature were found to be 0.88, 3.5, 37.2, and 36 cP, respectively. The estimated shear rate during the lubrication experiments is always in the range of 200–5000 s^{-1} , calculated by assuming that the distance between two sliding cartilages is 1 μm , which corresponds to the surface roughness of cartilage.²⁰ The sliding speed of our lubrication experiments is in the range of 0.2–5 mm/s.

Experimental Protocol: Friction Coefficient Experiments

The friction coefficient under a continuous static normal load of 2 N (corresponding to a nominal contact pressure of 0.63 MPa) was measured using a pin-on-disk tribometer (CSM, model S/N 18-312). The contact stress is within the physiological range during human walking activities.⁵¹ A schematic of the experimental set-up is shown in Fig. 1. All the tests began 5 s after applying the load. The samples were immersed in a liquid bath during the test. The disk rotated with a constant sliding velocity of 0.2, 0.5, 1, and 5 mm/s, depending on the experiment.

Friction coefficients were measured in the CA, CC, and AC testing configurations. A schematic of the

three testing configurations is shown in the bottom panel of Fig. 1. The alumina disk was aluminum, while the pin was ceramic alumina. All the experiments with lubricants dissolved in PBS were performed under the AC testing configuration, which, according to our results, better mimics physiological conditions compared to the CA testing configuration.

The friction coefficient between the contact surfaces was monitored continuously by measuring the deflection of the elastic arm that holds the pin. The data were collected as a function of time using the CSM ModelX software with an acquisition frequency of 10 Hz. All tests were performed by placing the pin-on-disk at a distance $r = 3 \pm 0.05$ mm from the center of the rotating plate. The experiments performed in PBS for AC, CC, and AC testing configurations were terminated after 100 laps with a constant sliding speed of 1 mm/s, corresponding to a traveled distance of 1885 mm. The tests conducted with lubricants (PEG or CS) dissolved in PBS were terminated after 20 laps, corresponding to a traveled distance of 377 mm (our results reveal that the friction coefficient does not change after 20 laps under the AC testing configuration). During one lap the friction coefficient shows a cyclic variation, which is due in part to the unevenness of the prepared sample, and, in large part, to intrinsic

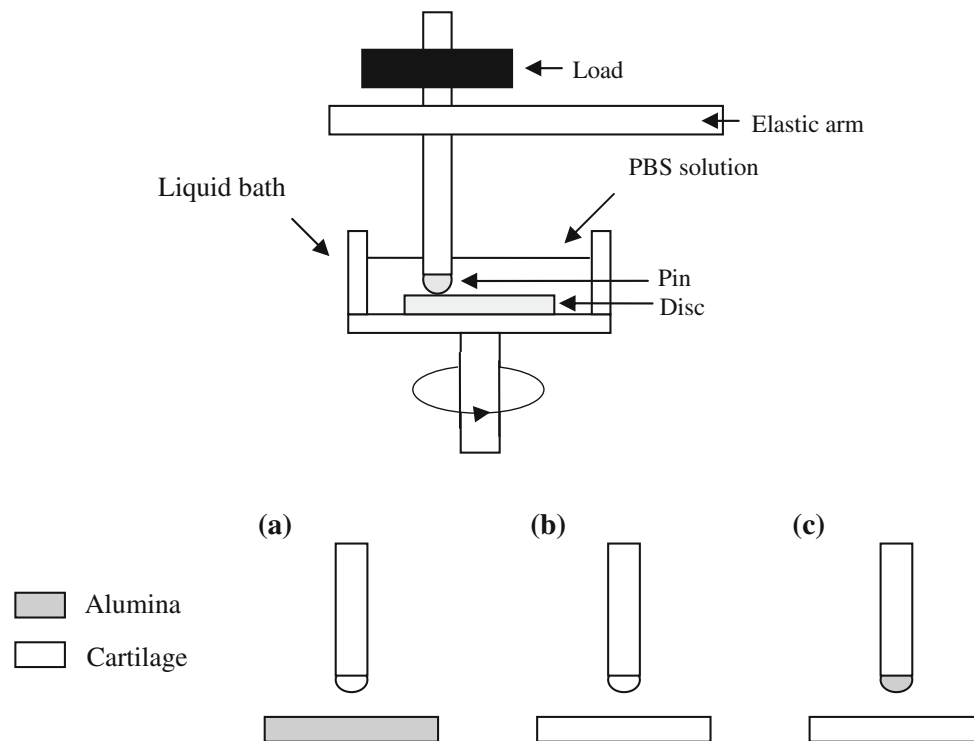


FIGURE 1. Schematic diagram of the pin-on-disk tribometer used in this study (top). The samples were immersed in PBS solutions during the experiment. The disk, together with the liquid bath, rotates with a constant velocity. The friction coefficient between pin and disk is monitored continuously by measuring the deflection of the elastic arm. On the bottom panel three testing configurations are represented: (a) CA; (b) CC; (c) AC.

vibrations experienced by the instrument elastic arm during the operation. The average friction coefficient in each lap is reported in what follows. All experiments were performed at room conditions. For each test the data reported herein are the average from ten independent measurements conducted at the same conditions.

We measured the contact area in the AC testing configuration by dyeing the pin (alumina sphere) and then measuring the colored trace on the cartilage glued on the disk. The contact area was found to have an average width of ~ 2 mm. To keep the contact area consistent when experiments are performed on the various testing configurations of Fig. 1, we cut the cartilages glued on the pin (alumina sphere) into plugs of diameter 2 mm. Because the size of the contact interface, ~ 2 mm, is much smaller than the size of the spherical support on the pin, which has a diameter of 8 mm, we can reasonably assume that the contact interfaces are flat for all the cases considered herein. Etsion and coworkers^{10,45} developed a theoretical model to study the effect of dwell time on the junction growth of a creeping polymer sphere in contact with a rigid flat surface, which may represent a spherical cartilage surface pressed onto a flat metal surface. According to Etsion *et al.* model, the contact interface does not change during our experiment, because of the low applied pressures.⁵¹ We also conducted one test experiment under the CA testing configuration in which the cartilage sample was glued on a flat pin. Results did not differ qualitatively from those obtained using a spherical support on the pin.

Cartilage Surface Characterization

Following examples from literature,^{23,37,64,65} SEM has been used to characterize articular cartilage surfaces. Specimens were fixed in 2% glutaraldehyde and 0.1 M PBS for 24 h, following by further fixation in 1% osmium tetroxide for 1.5 h. Specimens were dehydrated using ethanol and critical-point dried with a Tousimis autosamdri-814 critical point drier. Then the Hummer VI sputtering system (Anatech Ltd.) was used to coat the cartilage specimen with 8 nm of gold. SEM images were obtained using a JEOL JSM-840A instrument before and after conducting our friction-coefficient experiments to visualize and quantify wear.

Data Interpretation

We applied the interstitial fluid pressurization model as proposed by Ateshian and coworkers to analyze our results for the measured time-dependent friction

coefficient μ_{eff} under different testing configurations. Although immature bovine specimens were used to derive Eq. (1), it should be remembered that McCutchen⁴⁸ used mature shoulder leg pig cartilage samples when he originally demonstrated the importance of interstitial fluid support (weeping fluid lubrication). Our hypothesis is that the model can be applied to the friction coefficient measurement for healthy mature bovine cartilage specimens. Following Torzilli,⁶⁷ φ was considered equal to 0.1, corresponding to the solid content of the superficial zone of immature bovine articular cartilage. The model of Eq. (1) was proposed to analyze the friction coefficient measured in a friction device with intermittent linear sliding between the surfaces, under constant applied load. This testing configuration is similar to the CA testing configuration shown in Fig. 1. In this study we assume the model of Eq. (1) suitable to interpret the friction results obtained using not only the CA but also the CC and AC testing configurations. The accuracy of this assumption is assessed by comparing our experimental results to model fits.

All quantities in Eq. (1) are function of time, except μ_{eq} . Our experimental set-up allows us to measure $\mu_{\text{eff}}(t)$ as a function of constant load W . Unfortunately, we have no access to $W^P(t)$, the load supported by the interstitial fluid. However, we observe that according to Eq. (1) the measured friction coefficient increases as the load supported by the interstitial fluid W^P decreases. When $W^P = 0$, $\mu_{\text{eff}} = \mu_{\text{eq}}$. We assume that μ_{eq} obtained at the end of the CA testing configuration experiment corresponds to μ_{eq} also for the experiments conducted in the CC and AC testing configurations. Knowing this value, we can calculate $W^P(t)$ by Eq. (1) when the experimental $\mu_{\text{eff}}(t)$ is known. This procedure seems reasonable for the AC testing configuration, but μ_{eq} is expected to be somewhat lower in the CC configuration because two cartilage surfaces slide on each other.

Statistical Analysis

The mean and standard deviation were calculated and the statistical significance of the differences in friction coefficient was determined. A two-way analysis of variance (ANOVA) with Tukey's HSD post hoc test was used to compare the initial and steady-states friction coefficient values among different testing configurations. The effect of lubricant type and applied speed on the friction coefficient of cartilage was determined by a two-way ANOVA with Tukey's HSD post hoc test. All statistical analyses were carried out using PASW Statistics 18 (SPSS Inc., Chicago, IL, USA); α was set to be 0.05 and the statistical significance was accepted for $P < 0.05$.

RESULTS

SEM Images

We used SEM to characterize the cartilage surfaces before and after the friction experiment. Figures 2a and 2b show the 40° tilt and top view SEM images of an intact articular cartilage surface, respectively. The images show a smooth cartilage surface with some underlying chondrocytes, indicating a healthy and flat sample. Figure 2c is the top view of a cartilage sample after one experiment conducted in the AC testing configuration. Visual analysis reveals an abrasion on the surface due to the continuous sliding of the alumina ball onto the cartilage sample for 100 laps. The width of the abrasion (~2 mm) is consistent with our early estimation (see “[Experimental protocol: friction coefficient experiments](#)” section). Figure 2d is 40° tilt view SEM image at the intact-worn cartilage interface. The left side of this image is the intact cartilage, while the abrasion lies on the right of the broken line. The abrasion visualized by SEM is very shallow, suggesting that our experiments only produce minor wear on the cartilage samples probably because of the small applied load. All cartilage samples used for our studies appear smooth and healthy, suggesting that limited, if any, degradation has occurred before testing. The extent of wear due to conducting our experiments

appears limited. This could be further reduced if smooth alumina balls were used for the experiment. Because no experimental observation is available in the literature for cartilage wear under the experimental conditions considered herein, in particular when the AC testing configuration is implemented in a pin-on-disk tribometer, comparison regarding wear results is not possible. For completeness, we point out that when the experiments are conducted for longer times, the extent of wear increases. The cartilage samples eventually degrade if the experiments are conducted for 1 h or longer. These latter results are strongly dependent on the sample used. Statistical analysis of such results is beyond the scopes of this study.

To test the effect of unavoidable wear on the friction coefficient measured for cartilage during the experiment, we measured the friction coefficient for each cartilage plug twice under the same testing configuration. In-between the two experiments the cartilage plugs were allowed to relax in PBS solution for 2 h without applied load. The slight wear on the surface during the experiment shown by our SEM results shown in Fig. 2 was found to have limited effect on the measured friction coefficient. In very rare cases the friction coefficient measured in two experiments on the same cartilage sample showed large deviations. Data are presented here only if the measured friction

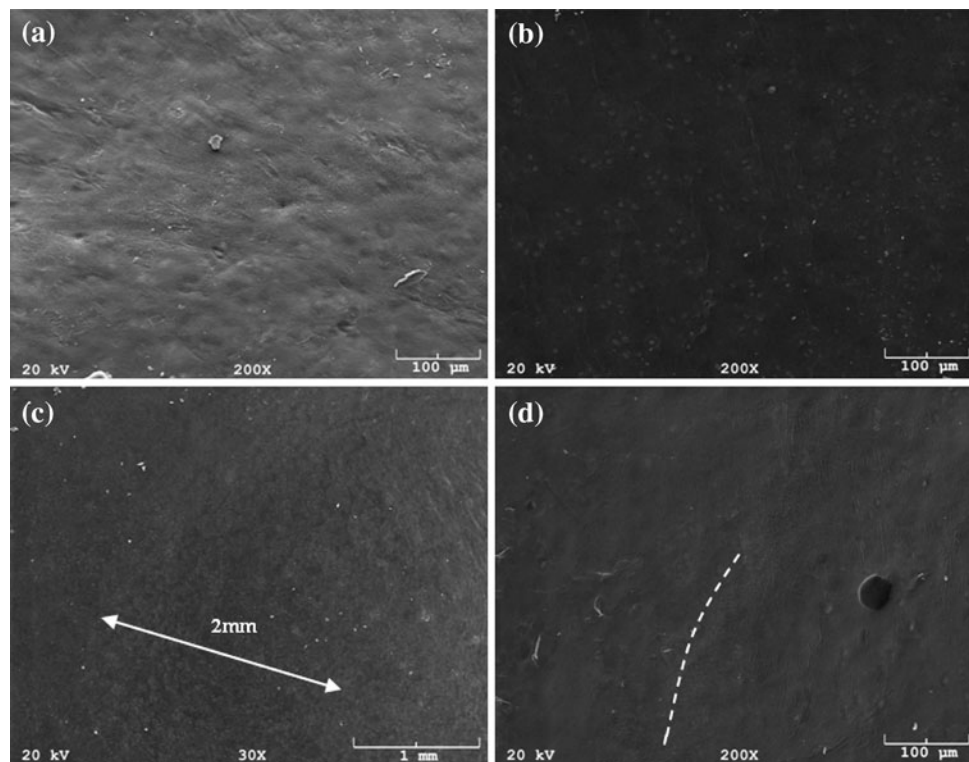


FIGURE 2. SEM images of intact and worn articular cartilage surfaces. (a) 40° tilt view of untreated cartilage; (b) top view of untreated cartilage; (c) top view of the worn area of cartilage after 100 laps; (d) 40° tilt view of the intact-worn interface of cartilage after 100 laps (the intact surface is on the left of the broken line).

coefficients from the two experiments are consistent ($\pm 10\%$).

Testing Configuration Effects

CA Testing Configuration

The experimental results for the friction coefficient and the corresponding fraction of load supported by the interstitial fluid in the CA testing configuration are shown in Fig. 3. The friction coefficient was found to increase with time from a minimum of $\sim 0.099 \pm 0.014$ to a plateau value of $\sim 0.271 \pm 0.015$. The plateau is reached within ~ 750 s after starting the experiment. According to the biphasic lubrication model of Eq. (1), as the measured friction coefficient increases the fraction of load supported by the interstitial fluid decreases from $\sim 71\%$ at the beginning of the experiment to ~ 0 at the end of it.

In Fig. 3 we also show the results obtained when a flat pin was used to hold a cartilage sample. These data, represented by the empty triangles, are consistent with those obtained using a sphere to support the cartilage (filled spheres). The only noticeable difference is that the friction coefficient at steady-states is slightly larger on the former than on the latter case. According to results reported by Merkher *et al.*,⁴⁹ this difference is consistent with a slightly larger contact area when the flat pin is used, despite the fact that a cartilage plug of 2 mm diameter was used in both experiments.

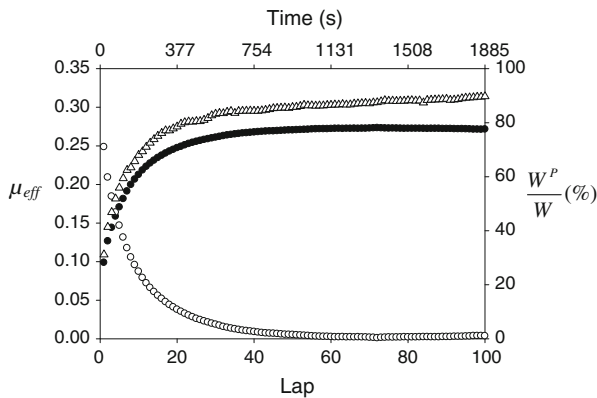


FIGURE 3. Time-dependent friction coefficient, μ_{eff} , and the portion of load supported by interstitial fluid, W^P/W , obtained in the CA testing configuration (see Fig. 1 for details). During the friction experiment 1885 s correspond to a sliding distance of 1.885 m and 100 laps. Filled circles are for the measured friction coefficient; empty circles are for the fraction of load supported by the interstitial fluid. Empty triangles are for the friction coefficient measured when the cartilage was supported by a flat pin. No estimation for the fraction of load supported by the interstitial fluid was attempted in the latter case. Error bars, not shown here for clarity, are included in Table 1.

CC Testing Configuration

In Fig. 4 we report the measured friction coefficient, as well as the estimated portion of load supported by interstitial fluid, obtained in the CC testing configuration. The shape of the friction coefficient curve is similar to that obtained under the CA testing configuration. However, at steady-states μ_{eff} (0.071 ± 0.017) is only $\sim 15\%$ larger than at the beginning of the experiment, when $\mu_{\text{eff}} \sim 0.062 \pm 0.021$. The corresponding fraction of load supported by the interstitial fluid, obtained assuming that μ_{eq} is equal to that measured in Fig. 3, remains high during the entire experiment. It decays from $\sim 86\%$ at the beginning of the experiment to $\sim 82\%$ in ~ 500 s, at steady states.

AC Testing Configuration

In Fig. 5 we report the measured friction coefficient, together with the estimated portion of load supported by the interstitial fluid, obtained in the AC testing configuration. The effective friction coefficient remains low during the whole experiment. The value reached at steady-states, $\sim 0.064 \pm 0.017$, is similar to that observed under the CC testing configuration (Fig. 4). The main difference between the result shown in Fig. 5 and those shown in Figs. 3 and 4 consists in the shape of the μ_{eff} vs. time curve. The measured friction coefficient starts from a relatively high value at the beginning of the experiment ($\sim 0.070 \pm 0.019$) and decreases with time to reach a plateau of $\sim 0.064 \pm 0.017$. Correspondingly, the estimated fraction of load supported by the interstitial fluid increases from ~ 82 to 85% .

In Table 1 we summarize the results presented in Figs. 3, 4, and 5 by reporting the friction coefficient measured at the beginning of each experiment, μ_{initial} , as well as the one observed at steady-states, μ_{eq} , for the

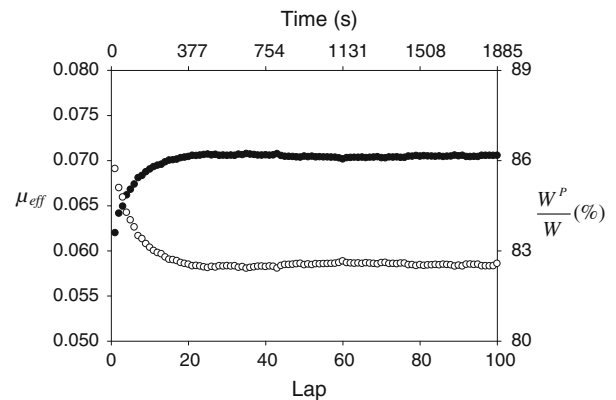


FIGURE 4. Time-dependent friction coefficient, μ_{eff} , and portion of load supported by interstitial fluid, W^P/W , measured in the CC testing configuration. Filled circles are for the measured friction coefficient; empty circles are for the fraction of load supported by the interstitial fluid. Error bars, not shown here for clarity, are included in Table 1.

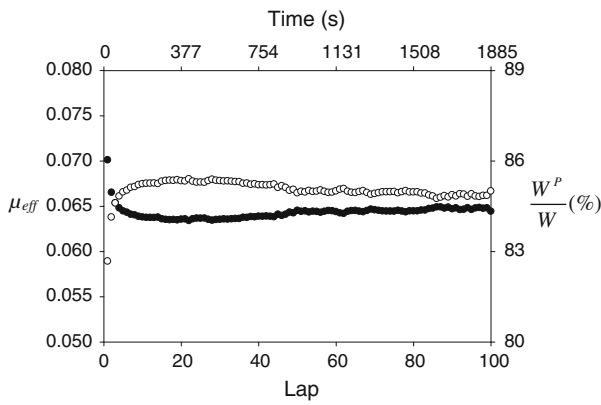


FIGURE 5. Time-dependent friction coefficient, μ_{eff} , and portion of load supported by interstitial fluid, W^P/W , measured in the AC testing configuration. Filled circles are for the measured friction coefficient; empty circles are for the fraction of load supported by the interstitial fluid. Error bars, not shown here for clarity, are included in Table 1.

TABLE 1. Initial and steady-states values for the measured friction coefficient (μ_{initial} and μ_{eq} , respectively) and for the estimated fraction of load supported by the interstitial fluid in the three testing configurations considered.

	CA	CC	AC
μ_{initial}	$0.099 \pm 0.014^\dagger$	$0.062 \pm 0.021^*$	$0.070 \pm 0.019^*$
μ_{eq}	$0.271 \pm 0.015^\dagger$	$0.071 \pm 0.017^{**}$	$0.064 \pm 0.017^{**}$
$(W^P/W)_{\text{initial}}$	$71\%^\dagger$	$86\%^*$	$82\%^*$
$(W^P/W)_{\text{eq}}$	$0\%^\dagger$	$82\%^{**}$	$85\%^{**}$

* $p < 0.01$ for CA vs. CC or AC; ** $p < 0.001$ for CA vs. CC or AC; † $p < 0.001$ for initial vs. steady states.

three testing configurations considered. We also report the estimated fraction of load supported by the interstitial fluid pressurization at the beginning of the experiment, $(W^P/W)_{\text{initial}}$, and at steady-states $(W^P/W)_{\text{eq}}$.

Lubricant and Sliding-Speed Effects

To understand the ability of different polymers dissolved within PBS to reduce the measured friction coefficient, we measured the friction coefficient of cartilage lubricated with four solutions: (1) PBS, which acts as control; (2) 100 mg/mL 10,000 MW PEG in PBS; (3) 100 mg/mL 100,000 MW PEG in PBS; and (4) 100 mg/mL CS in PBS. For these experiments we only considered the AC testing configuration, in which the alumina-on-pin slides on the cartilage-on-disk.

For brevity, we do not report each individual time-dependent μ_{eff} obtained with the four solutions at sliding speed of 1 mm/s and normal load of 2 N. All the curves follow the features described in Fig. 5. μ_{eff} , however, strongly depends on the lubricants. The

friction coefficients of cartilage lubricated with 100 mg/mL 100,000 MW PEG and 100 mg/mL CS in PBS are $\sim 40\%$ less than those measured in PBS both at the beginning of the experiment and at steady-states. Comparing the results obtained with PEG of different molecular weights, it is found that the high-molecular-weight PEG decreases the friction coefficient more significantly than the low-molecular-weight one does. This difference is due to the solution viscosity, which is 37.2 cP for the 100,000 MW PEG, but only 3.5 cP for the 10,000 MW PEG. Although PEG is very different than HA, it is interesting to point out that the importance of solution viscosity found in our experiments is consistent with the results reported by Mori *et al.*⁵⁰ Those researchers found that very viscous HA lubricants can decrease the friction coefficient of cartilage.

Because several literature reports revealed that friction coefficient for cartilage depends on sliding speed,^{22,49,70} we generated a mesh plot to investigate the friction coefficient, μ_{eff} , of cartilage in the four solutions just described over a range of sliding speeds (0.2, 0.5, 1, and 5 mm/s). For these experiments we only considered the AC testing configuration in which an alumina sphere slides on the cartilage sample. The results are described in the following sections.

Phosphate Buffered Saline

The friction coefficient of cartilage in PBS over a range of sliding speeds and lap number is reported in Fig. 6a. At any sliding speed, μ_{eff} changes as the lap number (traveled distance) increases, following the trend discussed in Fig. 5, i.e., μ_{eff} starts from a high value and decreases to a plateau within a few laps. The friction coefficient decreases as the sliding speed increases. The decrease in the measured μ_{eff} is more dramatic when the sliding speed increases from 0.2 to 1 mm/s, than in the high-speed range when the sliding speed reaches 5 mm/s. μ_{eff} decreases from the maximum of 0.095 ± 0.020 , obtained at the beginning of the experiment performed at the slowest sliding speed, 0.2 mm/s, to the minimum of 0.044 ± 0.016 at the end of the experiment conducted at the highest sliding speed, 5 mm/s.

100 mg/mL 10,000 MW PEG in PBS

The friction coefficient, μ_{eff} , of cartilage lubricated with 100 mg/mL 10,000 MW PEG in PBS over a range of sliding speeds and lap numbers is reported in Fig. 6b. The shape of the plot is similar to that observed in PBS (Fig. 6a). The friction coefficient of cartilage in 10,000 MW PEG solution is not significantly lower than that measured in PBS. μ_{eff} decreases

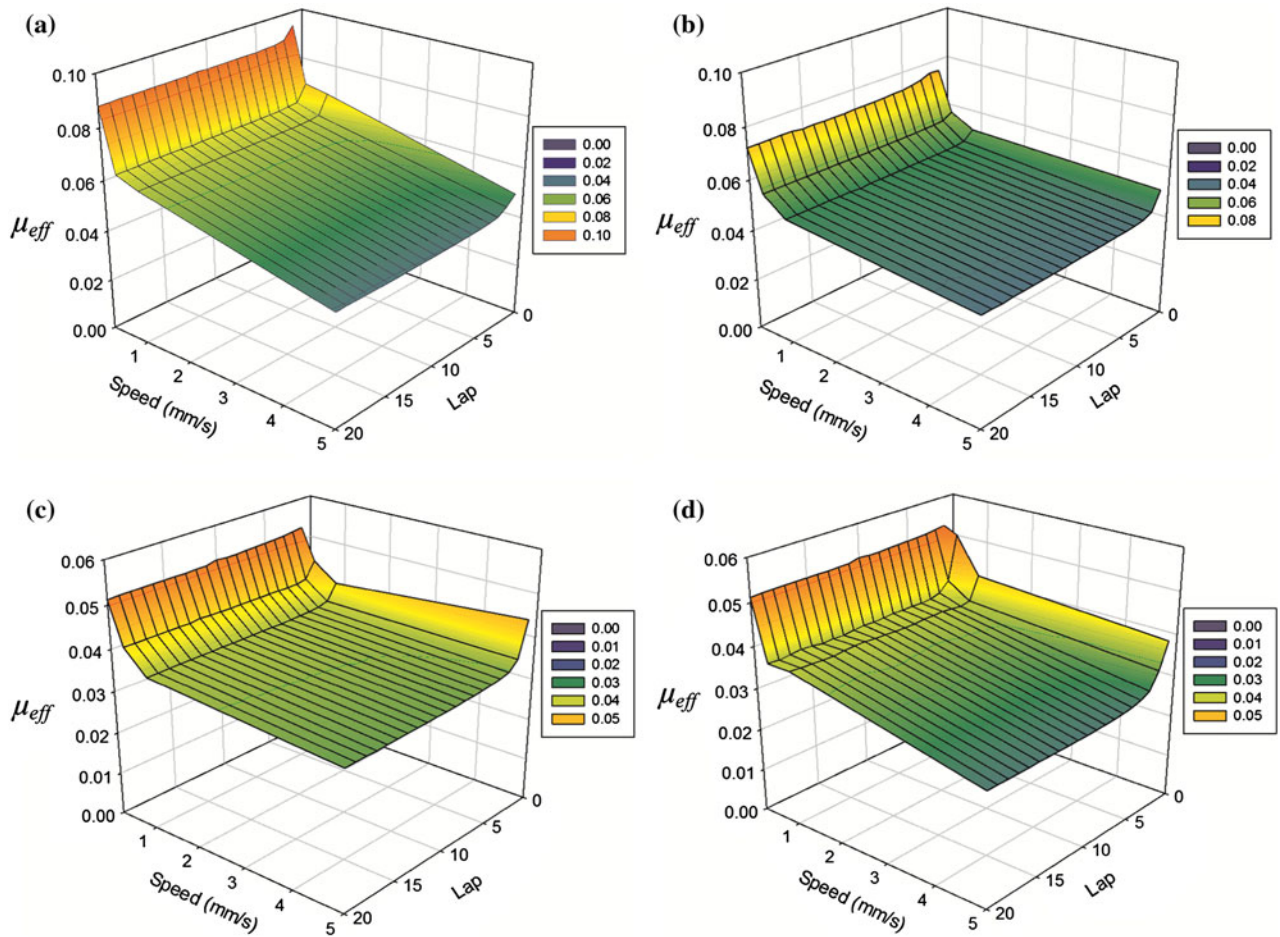


FIGURE 6. Friction coefficient, μ_{eff} , measured in the AC testing configuration over a range of sliding speeds and laps. (a) for cartilage lubricated with PBS; (b) for cartilage lubricated with 100 mg/mL 10,000 MW PEG in PBS; (c) for cartilage lubricated with 100 mg/mL 100,000 MW PEG in PBS; (d) for cartilage lubricated with 100 mg/mL CS in PBS. For clarity, error bars are not shown. The statistical analysis is summarized in Fig. 7.

from 0.076 ± 0.028 at the beginning of the experiment performed at the slowest sliding speed, 0.2 mm/s, to the minimum of 0.043 ± 0.020 at the end of the experiment conducted at the highest sliding speed, 5 mm/s.

100 mg/mL 100,000 MW PEG in PBS

The friction coefficient of cartilage lubricated with 100 mg/mL 100,000 MW PEG in PBS over a range of sliding speeds and lap numbers is reported in Fig. 6c. The plot follows the same trend observed from both PBS and 10,000 MW PEG solutions, although μ_{eff} is significantly lower than those reported above. μ_{eff} decreases from the maximum of 0.053 ± 0.012 obtained at the beginning of the experiment performed at the slowest sliding speed, 0.2 mm/s, to the minimum of 0.033 ± 0.010 at the end of the experiment conducted at 5 mm/s.

100 mg/mL CS in PBS

The friction coefficient of cartilage lubricated with 100 mg/mL CS in PBS is reported in Fig. 6d. The plot follows the trend discussed above. As the sliding speed increases above 2 mm/s the measured friction coefficient decreases only slightly. μ_{eff} decreases from the maximum of 0.064 ± 0.018 at the beginning of the experiment performed at the slowest sliding speed, 0.2 mm/s, to the minimum of 0.028 ± 0.003 at the end of the experiment conducted at the highest sliding speed, 5 mm/s.

DISCUSSION

Testing Configuration Effects

The first objective of our study is to assess testing configuration effects on the measured friction

coefficient for cartilage. A summary of our experimental results is reported in Table 1. The results from the CA testing configuration are consistent with previous results from McCutchen,⁴⁸ Ateshian,² and Krishnan *et al.*⁴¹ These results confirm that the interstitial fluid pressurization is a primary mechanism in the regulation of the friction response of articular cartilage at short times after a load is applied. As long as the interstitial fluid pressure remains high, the measured friction coefficient is low. When the pressure sustained by the interstitial fluid reduces to zero, the friction coefficient reaches its steady-states value.

We point out that the cartilage in our CA experiments is supported on a sphere, not on a flat pin. Although it is possible that as our experiment progresses the contact area changes due to deformation of the supported cartilage, geometrical considerations suggest that the contact area between cartilage on pin and disk is almost flat. Experiments conducted for a cartilage plug supported by a flat pin (see Fig. 3) confirm that our interpretation does not depend on the geometry of the pin.

More importantly, when the friction experiment is performed under the CC and AC testing configurations, the measured friction coefficient remains low during the entire experiment. The friction coefficient at steady-states (μ_{eq}) in these two configurations is ~25% that measured in the CA configuration. One reason for this low friction coefficient is the testing configuration itself. The CC and AC configurations allow cyclical loading on the cartilage. This type of loading, analogous to the migrating contact area discussed by Caligaris and Ateshian,¹² reasonably mimics the physiological conditions in diarthrodial joints, allowing the PBS solution to diffuse back into the cartilage before the load is applied again on the same contact area. For completeness, it should be pointed out that McCutchen⁴⁸ had also observed that allowing the cartilage to ‘resoak’ for a few seconds in-between friction experiments yields lower friction coefficients. Our CC and AC testing configurations allow the various cartilage regions compressed by the load to resoak before the load returns. Based on Eq. (1), the estimated fluid load support remains above 80% during the experiment in both CC and AC testing configurations. This result is in contrast to what observed for the CA testing configuration, in which case the friction coefficient rises significantly with time. This happens because in the CA configurations the constantly applied load on the cartilage forces the interstitial fluid to escape out of the cartilage matrix. As the loading time increases the interstitial fluid support decreases due to the lack of fluid phase.

The measured friction coefficient μ_{eff} increases with time for both the CA and CC testing configurations,

while it slightly decreases over time in the AC testing configuration. During the time in between when the load is applied and when the experiment starts (5 s), a certain amount of fluid escapes from the cartilage glued on the disk. Thus, the high onset friction coefficient in the AC testing configuration is likely due to the depletion of fluid phase in the contact area of cartilage on the disk. This possibility is consistent with the results reported by Forster and Fisher.²⁰ As the sliding distance increases, the fluid phase diffuses back to the pores present in the cartilage sample glued on the disk during the migrating contact area displacement, yielding lower steady-states friction coefficients.

Comparing CC and AC configurations, we propose that the CC configuration should obey the interstitial fluid pressurization mode, because it has a cartilage plug glued on the top, similarly to the experimental set-up of Krishnan’s work. In addition, according to Hlavacek,^{28–34} when the fluid is squeezed out of the cartilage under the CC configuration, it can diffuse back to both cartilage surfaces to perform its role as load support. The lubrication mechanism under the AC testing configuration may be different, because the solid alumina does not have pores that contain interstitial fluid. As the load is applied, the fluid squeezed out of cartilage into the region between alumina pin and the cartilage forms a temporary fluid film. Thus, it is possible that the low friction obtained in the AC testing configuration is in part to hydrodynamic lubrication (further evidence for this mechanism is provided in “[Lubricant and sliding-speed effects](#)” section).

The experimental procedure discussed above could be improved to extend results and methods to those attainable under physiological conditions. First, to limit the inevitable necrosis, the freshest cartilage samples available should be used. And second, the experiments could be conducted under a controlled temperature environment mimicking body temperature. It is possible that trimming the osteochondral plugs does not conserve structural integrity, leading to changes of cartilage physical properties. However, when large cartilage samples are trimmed and then glued on the disk of pin-on-disk instruments, the surface area subject to trimming tends to be far from that tested during the friction experiment. Experiments conducted under the AC testing configuration should not be affected by this limitation.

The applicability of the interstitial fluid pressurization model to interpret the results presented herein implies that lubrication in articular joints can be improved by increasing the load fraction supported by the interstitial fluid pressurization. More interestingly, our results indicate a different lubrication mechanism of cartilage under the AC testing configuration from

that of CA and CC testing configurations. The further study of the lubrication mechanism of cartilage under AC testing configuration could lead to better understanding cartilage lubrication.

Lubricant and Sliding-Speed Effects

We investigated how the presence of lubricants within the PBS solution, as well as changes in sliding speed, affect the measured friction coefficient. The comparison of initial and steady-states friction coefficients from different testing speeds and lubricants in PBS are reported in Figs. 7a and 7b, respectively. Because the AC configuration was used in all cases, the interstitial fluid supports part of the load in all cases, and the friction coefficients remain low. The initial friction coefficient is larger than the steady-states friction coefficient for all experiments, as discussed in “Testing configuration effects” section.

Both the initial and steady-states friction coefficients decrease as the sliding speed increases. This finding agrees with other reports, although the typical testing configuration adopted in those other reports was similar to our CA.^{22,49,70} This suggests that the effect of the sliding speed on the measured friction coefficient might be independent on the testing configuration.

Comparing the effects of lubricants, we find that both 100,000 MW PEG and CS, when dissolved within PBS, are very efficient lubricants for articular cartilage, since they reduce both initial and steady-states friction coefficients by ~40% (the effect appears stronger at slower sliding speeds). The ability of 10,000 MW PEG to reduce the friction coefficient is less pronounced. Literature data agree in that CS lowers the friction coefficient measured for cartilage.^{6,9,40} However, it should be pointed out that these literature reports refer

to experiments conducted under conditions, comparable to the CA testing configuration, in which boundary lubrication is expected. Our results for PEG disagree in part with those reported by Basalo *et al.*,⁶ who observed that PEG solutions reduce the friction coefficient for cartilage independently on their viscosity. The difference between ours and Basalo *et al.*'s findings could be due either to the difference of testing configuration implemented, or to the molecular weight of PEG used. Basalo *et al.* conducted their experiments under a CA configuration, whereas our data are obtained under the AC configuration. As we discussed in “Testing configuration effects” section, these two testing configurations could promote different lubrication mechanisms. More important, however, is that Basalo *et al.*⁶ changed the viscosity of the PBS solution by dissolving different amounts of 20,000 MW PEG in PBS. Consequently, the viscosities in Basalo *et al.*'s work ranged from 16.7 cP (133 mg PEG/mL of solution) to 24.4 cP (170 mg/mL). By changing the PEG molecular weight, we increased the PBS solutions viscosity from 3.5 cP (10,000 MW PEG) to 37.2 cP (100,000 MW PEG). Although it is possible that the PEG molecular weight affects the lubrication mechanisms, it is likely that Basalo *et al.* did not observe significant changes in the measured friction coefficient because the viscosity of their solutions did not change significantly.

To further analyze our results, in Fig. 8 we plot the steady-states friction coefficient, μ_{eq} in Fig. 7b, as a function of the Hersey number, $\eta v/N$. In this analysis η is the zero-shear-rate viscosity of the corresponding lubricant PBS solution; v the sliding velocity; N the static normal load. The fact that all experimental data collapse into a single curve demonstrates the importance of solution viscosity, normal load, and sliding

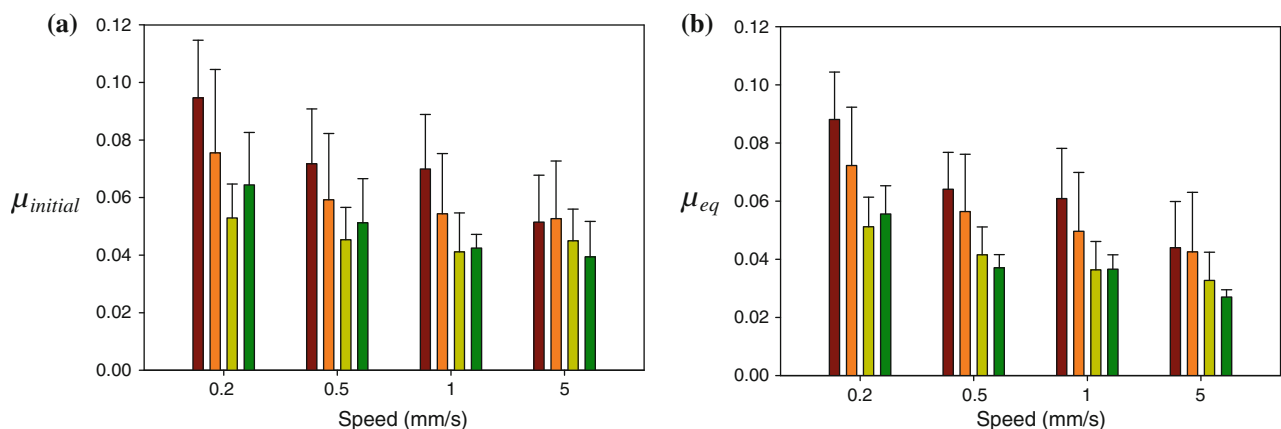


FIGURE 7. Comparison of the friction coefficient measured in the AC testing configuration when cartilage was lubricated with four different PBS solutions. Maroon represents PBS; orange represents 100 mg/mL 10,000 MW PEG in PBS; yellow represents 100 mg/mL 100,000 MW PEG in PBS; green represents 100 mg/mL CS in PBS. (a) initial friction coefficient, $\mu_{initial}$; (b) steady-states friction coefficient, μ_{eq} . $p < 0.05$ for 0.2 mm/s vs. other speed; $p < 0.05$ for PBS vs. other lubricants.

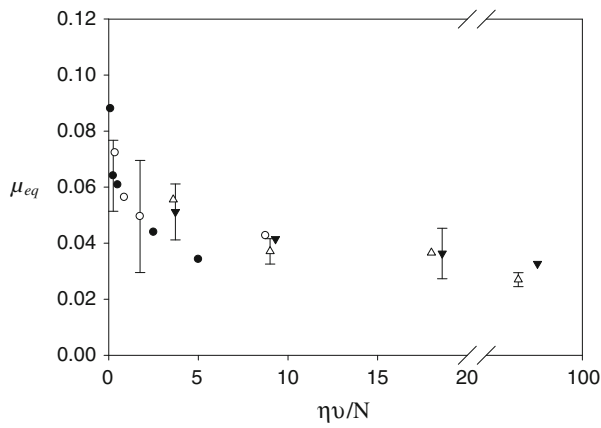


FIGURE 8. Stribeck curve obtained plotting the steady-states friction coefficient, μ_{eq} , measured in the AC testing configuration, as a function of the Hersey number ($\eta v/N$). Filled circles are for experiments conducted in PBS; empty circles are data obtained when 100 mg/mL 10,000 MW PEG is dissolved in PBS; filled inverted triangles are for 100 mg/mL 100,000 MW PEG in PBS; empty triangles are for 100 mg/mL CS in PBS. Only representative error bars are shown for clarity.

speed in determining cartilage lubrication. The curve in Fig. 8 can be divided in two parts. In the first part, μ_{eq} decreases as the Hersey number increases, indicating a ‘mixed lubrication region’ where boundary and fluid film lubrication mechanisms act simultaneously. At these conditions lubrication depends on both surface chemistry (boundary lubrication) and fluid hydrodynamics. In the second part, μ_{eq} does not change much as the Hersey number increases, indicating that, although both hydrodynamics and boundary lubrication mechanisms act simultaneously, hydrodynamics effects become more important.

The plot of Fig. 8 is consistent with the classical Stribeck curve, except that even at very low speeds (0.2 mm/s) and solution viscosities (0.88 cP for PBS), i.e., at very low Hersey numbers, our curve does not show a ‘boundary-mode region’ in which μ is invariant as the Hersey number changes. This observation provides further evidence to support our early discussion according to which a fluid film probably exists under the AC testing configuration at all conditions considered herein. Because a fluid film may prevent the direct interaction of the two surfaces, no boundary lubrication region is observed in Fig. 8. Gleghorn and Bonassar²² reported a boundary region in their findings. This disagreement is due to the different testing configurations employed and the different lubrication mechanisms that prevail under the various testing configurations. The data of Gleghorn and Bonassar²² were collected at steady-states using a CA configuration. It is likely that Gleghorn and Bonassar²² data show a boundary region in the Stribeck plot because the CA configuration leads to direct contact between

cartilage and disk when the interstitial fluid is dissipated at steady-states. In our work, at steady-states the cartilage glued on the disk always contains enough fluid to maintain a fluid film at the migrating contact area and no boundary region is observed. Our results suggest that experiments conducted in the AC testing configuration (this study) provide a complementary understanding of cartilage lubrication when combined with experiments conducted in configurations consistent with the CA testing configuration (e.g., the contribution by Gleghorn and Bonassar²²). It is however possible that changing the Hersey number by increasing the normal load (not attempted herein) could trigger to a larger extent the boundary lubrication mechanism, which is not evident from our results. Another difference between the curve in Fig. 8 and the classical Stribeck curve is that the friction coefficient in our experiments does not increase slowly as Hersey number reaches very high values, as expected should hydrodynamic lubrication be the only acting mechanism. This suggests that, within the experimental conditions tested herein, the fluid hydrodynamics under the AC configuration never determine the lubrication mechanism of articular cartilage by itself.

CONCLUSIONS

The friction coefficient between cartilage surfaces was measured using a pin-on-disk tribometer at constant load of 2 N at room conditions. No significant damage of the articular cartilage was observed from SEM images. Friction coefficients from different testing configurations (CA, CC, AC) and solutions (PBS; 10,000 MW PEG in PBS; 100,000 MW PEG in PBS; CS in PBS) were compared. Fitting of our experimental data obtained in CA and CC testing configurations is possible using a model that accounts for the support provided by the interstitial fluid.

The measured friction coefficient strongly depends on the testing configuration, suggesting that using a commercial pin-on-disk tribometer and by controlling the experimental set-up different lubrication mechanisms can be assessed. The most interesting conclusion is that the friction coefficient measured when cartilage is glued on the disk remains very low as the experiment proceeds, probably because as the pin moves on the cartilage surface (migrating contact area) the pores present in cartilage, although depleted of PBS solution when the load is applied, replenish before the load is applied again on the same area. As a consequence the fluid phase supports a large fraction of the applied load, and the friction coefficient remains low. These results suggest that the AC testing configuration could be used to assess wear-and-tear characteristics of

materials used in prosthetic devices (which should be supported on the pin), as well as possible implants designed to improve lubrication in articular joints. Based on our analysis, it is expected that when the AC testing configuration is implemented lubrication is provided, in part, by hydrodynamics fluid film and by interstitial fluid support mechanisms.

The measured friction coefficients, obtained under the AC testing configuration, strongly depend on sliding speed and solution viscosity. We found that 100 mg/mL of either CS or 100,000 MW PEG dissolved in PBS can reduce the friction coefficient of articular cartilage by ~40% compared to results obtained in PBS. These results suggest that high-molecular-weight polymers of low or no toxicity (e.g., PEO) could be used to aid the lubrication of prosthetic joints.

When the steady-states friction coefficient obtained in the AC testing configuration are plotted as a function of the Hersey number, our results are consistent with a Stribeck curve, indicating that the friction coefficient of cartilage depends on the solution zero-shear viscosity, η , sliding velocity, v , and normal load, N . Because of the testing configuration implemented, at all conditions the lubricant solution, partially adsorbed within the cartilage pores, supports part of the applied load, leading to low friction coefficients. Comparing our data with available literature reports, we identify experimental conditions under which various mechanisms (hydrodynamic, boundary, fluid film) dominate cartilage lubrication. However, even at very high Hersey numbers we do not observe evidence supporting hydrodynamics-only lubrication, suggesting that multiple lubrication modes are always simultaneously responsible for the low friction coefficient observed for articular cartilage under the conditions assessed in our experiments.

ACKNOWLEDGMENTS

Funding for this project was kindly provided by the Oklahoma Center for the Advancement of Science and Technology (OCAST), by the Oklahoma Regents for Higher Education, and by the Vice President for Research at the University of Oklahoma.

REFERENCES

- ¹Ateshian, G. A. A theoretical formulation for boundary friction in articular cartilage. *J. Biomech. Eng. Trans. ASME* 119(1):81–86, 1997.
- ²Ateshian, G. A. The role of interstitial fluid pressurization in articular cartilage lubrication. *J. Biomech.* 42(9):1163–1176, 2009.
- ³Ateshian, G. A., W. M. Lai, W. B. Zhu, and V. C. Mow. An asymptotic solution for the contact of 2 biphasic cartilage layers. *J. Biomech.* 27(11):1347–1360, 1994.
- ⁴Ateshian, G. A., and H. Wang. Rolling resistance of articular cartilage due to interstitial fluid flow. *Proc. Inst. Mech. Eng. H* 211(5):419–424, 1997.
- ⁵Ateshian, G. A., W. H. Warden, J. J. Kim, R. P. Grelsamer, and V. C. Mow. Finite deformation biphasic material properties of bovine articular cartilage from confined compression experiments. *J. Biomech.* 30(11–12): 1157–1164, 1997.
- ⁶Basalo, I. M., N. O. Chahine, M. Kaplun, F. H. Chen, C. T. Hung, and G. A. Ateshian. Chondroitin sulfate reduces the friction coefficient of articular cartilage. *J. Biomech.* 40(8):1847–1854, 2007.
- ⁷Bell, C. J., E. Ingham, and J. Fisher. Influence of hyaluronic acid on the time-dependent friction response of articular cartilage under different conditions. *Proc. Inst. Mech. Eng. H* 220(H1):23–31, 2006.
- ⁸Benz, M., N. H. Chen, G. Jay, and J. I. Israelachvili. Static forces, structure and flow properties of complex fluids in highly confined geometries. *Ann. Biomed. Eng.* 33(1):39–51, 2005.
- ⁹Bian, L. M., M. Kaplun, D. Y. Williams, D. Xu, G. A. Ateshian, and C. T. Hung. Influence of chondroitin sulfate on the biochemical, mechanical and frictional properties of cartilage explants in long-term culture. *J. Biomech.* 42(3): 286–290, 2009.
- ¹⁰Brizmer, V., Y. Kligerman, and I. Etsion. Elastic-plastic spherical contact under combined normal and tangential loading in full stick. *Tribol. Lett.* 25(1):61–70, 2007.
- ¹¹Buckwalter, J. A. Osteoarthritis and articular-cartilage use, disuse, and abuse-experimental studies. *J. Rheumatol. Suppl.* 43S:13–15, 1995.
- ¹²Caligaris, M., and G. A. Ateshian. Effects of sustained interstitial fluid pressurization under migrating contact area, and boundary lubrication by synovial fluid, on cartilage friction. *Osteoarthritis Cartilage* 16(10):1220–1227, 2008.
- ¹³Chan, S. M. T., C. P. Neu, G. DuRaine, K. Komvopoulos, and A. H. Reddi. Atomic force microscope investigation of the boundary-lubricant layer in articular cartilage. *Osteoarthritis Cartilage* 18(7):956–963, 2010.
- ¹⁴Charnley, J. The lubrication of animal joints in relation to surgical reconstruction by arthroplasty. *Ann. Rheum. Dis.* 19(1):10–19, 1960.
- ¹⁵Dean, D., L. Han, C. Ortiz, and A. J. Grodzinsky. Nano-scale conformation and compressibility of cartilage aggregate using microcontact printing and atomic force microscopy. *Macromolecules* 38(10):4047–4049, 2005.
- ¹⁶Dowson, D. Elastohydrodynamic and micro-elastohydrodynamic lubrication. *Wear* 190(2):125–138, 1995.
- ¹⁷Dowson, D. New joints for the Millennium: wear control in total replacement hip joints. *Proc. Inst. Mech. Eng. H* 215(H4):335–358, 2001.
- ¹⁸DuRaine, G., C. P. Neu, S. M. Chan, K. Komvopoulos, R. K. June, and A. H. Reddi. Regulation of the friction coefficient of articular cartilage by TGF- β 1 and IL-1 β . *J. Orthop. Res.* 27(2):249–256, 2009.
- ¹⁹Forsey, R. W., J. Fisher, J. Thompson, M. H. Stone, C. Bell, and E. Ingham. The effect of hyaluronic acid and phospholipid based lubricants on friction within a human

- cartilage damage model. *Biomaterials* 27(26):4581–4590, 2006.
- ²⁰Forster, H., and J. Fisher. The influence of loading time and lubricant on the friction of articular cartilage. *Proc. Inst. Mech. Eng. H* 210(2):109–119, 1996.
- ²¹Forster, H., and J. Fisher. The influence of continuous sliding and subsequent surface wear on the friction of articular cartilage. *Proc. Inst. Mech. Eng. H* 213(4):329–345, 1999.
- ²²Gleghorn, J. P., and L. J. Bonassar. Lubrication mode analysis of articular cartilage using Stribeck surfaces. *J. Biomech.* 41(9):1910–1918, 2008.
- ²³Graindorge, S. L., and G. W. Stachowiak. Changes occurring in the surface morphology of articular cartilage during wear. *Wear* 241(2):143–150, 2000.
- ²⁴Green, G. Understanding NSAIDs: from aspirin to COX-2. *Clin. Cornerstone* 3(5):50–60, 2001.
- ²⁵Helmick, C. G., D. T. Felson, R. C. Lawrence, S. Gabriel, R. Hirsch, C. K. Kwoh, M. H. Liang, H. M. Kremers, M. D. Mayes, and P. A. Merkel. Estimates of the prevalence of arthritis and other rheumatic conditions in the United States: Part I. *Arthritis Rheumat.* 58(1):15–25, 2008.
- ²⁶Hersey, M. D. Laws of lubrication. *J. Washington Acad. Sci.* 4:542–552, 1914.
- ²⁷Higginso, G. R., and R. Norman. Model investigation of squeeze-film lubrication in animal joints. *Phys. Med. Biol.* 19(6):785–792, 1974.
- ²⁸Hlavacek, M. The role of synovial-fluid filtration by cartilage in lubrication of synovial joints. 1. Mixture model of synovial-fluid. *J. Biomech.* 26(10):1145–1150, 1993.
- ²⁹Hlavacek, M. The role of synovial-fluid filtration by cartilage in lubrication of synovial joints. 2. Squeeze-film lubrication-homogeneous filtration. *J. Biomech.* 26(10):1151–1160, 1993.
- ³⁰Hlavacek, M. The role of synovial-fluid filtration by cartilage in lubrication of synovial joints. 4. Squeeze-film lubrication—the central film thickness for normal and inflammatory synovial-fluid for axial symmetry under high loading conditions. *J. Biomech.* 28(10):1199–1205, 1995.
- ³¹Hlavacek, M. Squeeze-film lubrication of the human ankle joint with synovial fluid filtrated by articular cartilage with the superficial zone worn out. *J. Biomech.* 33(11):1415–1422, 2000.
- ³²Hlavacek, M. The thixotropic effect of the synovial fluid in squeeze-film lubrication of the human hip joint. *Biorheology* 38(4):319–334, 2001.
- ³³Hlavacek, M. Squeeze-film lubrication of the human ankle joint subjected to the cyclic loading encountered in walking. *J. Tribol. Trans. ASME* 127(1):141–148, 2005.
- ³⁴Hlavacek, M., and J. Novak. The role of synovial-fluid filtration by cartilage in lubrication of synovial joints. 3. Squeeze-film lubrication-axial symmetry under low loading conditions. *J. Biomech.* 28(10):1193–1198, 1995.
- ³⁵Jay, G. D., U. Tantravahi, D. E. Britt, H. J. Barrach, and C. J. Cha. Homology of lubricin and superficial zone protein (SZP): products of megakaryocyte stimulating factor (MSF) gene expression by human synovial fibroblasts and articular chondrocytes localized to chromosome 1q25. *J. Orthop. Res.* 19(4):677–687, 2001.
- ³⁶Jay, G. D., J. R. Torres, D. K. Rhee, H. J. Helminen, M. M. Hytinen, C. Chung-Ja, K. Elsaid, K. Kyung-Suk, C. Yajun, and M. L. Warman. Association between friction and wear in diarthrodial joints lacking lubricin. *Arthritis Rheum.* 56(11):3662–3669, 2007.
- ³⁷Kääb, M. J., H. J. Bail, A. Rotter, P. Mainil-Varlet, L. Apgwynn, and A. Weiler. Monopolar radiofrequency treatment of partial-thickness cartilage defects in the sheep knee joint leads to extended cartilage injury. *Am. J. Sports Med.* 33(10):1472–1478, 2005.
- ³⁸Katta, J., Z. M. Jin, E. Ingham, and J. Fisher. Biotribology of articular cartilage—a review of the recent advances. *Med. Eng. Phys.* 30(10):1349–1363, 2008.
- ³⁹Katta, J., Z. Jin, E. Ingham, and J. Fisher. Effect of nominal stress on the long term friction, deformation and wear of native and glycosaminoglycan deficient articular cartilage. *Osteoarthritis Cartilage* 17(5):662–668, 2009.
- ⁴⁰Katta, J., Z. Jin, E. Ingham, and J. Fisher. Chondroitin sulphate: an effective joint lubricant? *Osteoarthritis Cartilage* 17(8):1001–1008, 2009.
- ⁴¹Krishnan, R., M. Kopacz, and G. A. Ateshian. Experimental verification of the role of interstitial fluid pressurization in cartilage lubrication. *J. Orthop. Res.* 22(3):565–570, 2004.
- ⁴²Krishnan, R., E. N. Mariner, and G. A. Ateshian. Effect of dynamic loading on the frictional response of bovine articular cartilage. *J. Biomech.* 38(8):1665–1673, 2005.
- ⁴³MacConaill, M. A. The function of inter-articular fibrocartilages, with special references to the knee and inferior radio-ulnar joints. *J. Anat.* 66:210–227, 1932.
- ⁴⁴Macirowski, T., S. Tepic, and R. W. Mann. Cartilage stresses in the human hip-joint. *J. Biomech. Eng. Trans. ASME* 116(1):10–18, 1994.
- ⁴⁵Malamut, S., Y. Kligerman, and I. Etsion. The effect of dwell time on the static friction in creeping elastic-plastic polymer spherical contact. *Tribol. Lett.* 35(3):159–170, 2009.
- ⁴⁶McCutchen, C. W. Boundary lubrication by synovial fluid—demonstration and possible osmotic explanation. *Federation Proc.* 25(3P1):1061–1068, 1966.
- ⁴⁷McCutchen, C. W. Sponge-hydrostatic and weeping bearings. *Nature* 184(4695):1284–1285, 1959.
- ⁴⁸McCutchen, C. W. The frictional properties of animal joints. *Wear* 5:1–17, 1962.
- ⁴⁹Merkher, Y., S. Sivan, I. Etsion, A. Maroudas, G. Halperin, and A. Yosef. A rational human joint friction test using a human cartilage-on-cartilage arrangement. *Tribol. Lett.* 22(1):29–36, 2006.
- ⁵⁰Mori, S., M. Naito, and S. Moriyama. Highly viscous sodium hyaluronate and joint lubrication. *Int. Orthop.* 26(2):116–121, 2002.
- ⁵¹Morrell, K. C., W. A. Hodge, D. E. Krebs, and R. W. Mann. Corroboration of in vivo cartilage pressures with implications for synovial joint tribology and osteoarthritis causation. *Proc. Natl Acad. Sci. USA* 102(41):14819–14824, 2005.
- ⁵²Mow, V. C., M. H. Holmes, and W. M. Lai. Fluid transport and mechanical-properties of articular-cartilage—a review. *J. Biomech.* 17(5):377–394, 1984.
- ⁵³Mow, V. C., S. C. Kuei, W. M. Lai, and C. G. Armstrong. Biphasic creep and stress-relaxation of articular-cartilage in compression—theory and experiments. *J. Biomech. Eng. Trans. ASME* 102(1):73–84, 1980.
- ⁵⁴Naka, M. H., Y. Morita, and K. Ikeuchi. Influence of proteoglycan contents and of tissue hydration on the frictional characteristics of articular cartilage. *Proc. Inst. Mech. Eng. H* 219(H3):175–182, 2005.
- ⁵⁵Neu, C. P., A. Khalafi, K. Komvopoulos, T. M. Schmid, and A. H. Reddi. Mechanotransduction of bovine articular cartilage superficial zone protein by transforming growth factor β signaling. *Arthritis Rheum.* 56(11):3706–3714, 2007.
- ⁵⁶Northwood, E., and J. A. Fisher. Multi-directional in vitro investigation into friction, damage and wear of innovative

- chondroplasty materials against articular cartilage. *Clin. Biomech.* 22(7):834–842, 2007.
- ⁵⁷Northwood, E., J. Fisher, and R. Kowalski. Investigation of the friction and surface degradation of innovative chondroplasty materials against articular cartilage. *Proc. Inst. Mech. Eng. H* 221(H3):263–279, 2007.
- ⁵⁸Oloyede, A., and N. Broom. Stress-sharing between the fluid and solid components of articular cartilage under varying rates of compression. *Connect. Tissue Res.* 30(2): 127–141, 1993.
- ⁵⁹Park, S. H., R. Krishnan, S. B. Nicoll, and G. A. Ateshian. Cartilage interstitial fluid load support in unconfined compression. *J. Biomech.* 36(12):1785–1796, 2003.
- ⁶⁰Paul, J. P., and D. A. McGrouther. Forces transmitted at the hip and knee joint of normal and disabled persons during a range of activities. *Acta Orthopaedica Belgica* 1(1):78–88, 1975.
- ⁶¹Pickard, J. E., J. Fisher, E. Ingham, and J. Egan. Investigation into the effects of proteins and lipids on the frictional properties of articular cartilage. *Biomaterials* 19(19): 1807–1812, 1998.
- ⁶²Radin, E. L., D. A. Swann, and P. A. Weisser. Separation of a hyaluronate-free lubricating fraction from synovial fluid. *Nature* 228(5269):377–378, 1970.
- ⁶³Sarma, A. V., G. L. Powell, and M. LaBerge. Phospholipid composition of articular cartilage boundary lubricant. *J. Orthop. Res.* 19(4):671–676, 2001.
- ⁶⁴Shields, K. J., J. R. Owen, and J. S. Wayne. Biomechanical and biotribological correlation of induced wear on bovine femoral condyles. *J. Biomech. Eng.* 131(6):061005, 2009.
- ⁶⁵Stachowiak, G. P., G. W. Stachowiak, and P. Podsiadlo. Automated classification of articular cartilage surfaces based on surface texture. *Proc. Inst. Mech. Eng. H* 220(8): 831–843, 2006.
- ⁶⁶Tanaka, E., T. Iwabe, D. A. Dalla-Bona, N. Kawai, T. van Eijden, M. Tanaka, and K. Tanne. The effect of experimental cartilage damage and impairment and restoration of synovial lubrication on friction in the temporomandibular joint. *J. Orofac. Pain* 19(4):331–336, 2005.
- ⁶⁷Torzilli, P. A. Water-content and equilibrium water partition in immature cartilage. *J. Orthop. Res.* 6(5):766–769, 1988.
- ⁶⁸Van, C., and W. C. Mow. Chapter 4 ‘Structure and Function of Articular Cartilage and Meniscus’ Basic Orthopaedic Biomechanics (2nd ed.). Philadelphia: Lippincott Williams, 1997.
- ⁶⁹Walker, P. S., D. Dowson, M. D. Longfiel, and V. Wright. Boosted lubrication in synovial joints by fluid entrapment and enrichment. *Ann. Rheum. Dis.* 27(6):512–518, 1968.
- ⁷⁰Williams, III, P. F., G. L. Powell, and M. LaBerge. Sliding friction analysis of phosphatidylcholine as a boundary lubricant for articular cartilage. *Proc. Inst. Mech. Eng. H* 207(1):59–66, 1993.